

Contents lists available at [ScienceDirect](https://www.sciencedirect.com)

## Journal of Sound and Vibration

journal homepage: [www.elsevier.com/locate/jsv](http://www.elsevier.com/locate/jsv)

## FRF-based finite element model updating for non-viscous and non-proportionally damped systems

Vikas Arora<sup>a,\*</sup>, Sondipon Adhikari<sup>b</sup>, Kiran Vijayan<sup>c</sup><sup>a</sup> Department of Mechanical and Electrical Engineering, University of Southern Denmark, Campusvej 55, Odense 5230, Denmark<sup>b</sup> James Watt School of Engineering, The University of Glasgow, Glasgow, UK<sup>c</sup> Department of Ocean Engineering and Naval Architecture, IIT Kharagpur, 721302, India

## ARTICLE INFO

## Keywords:

Non-proportional and non-viscous damping  
 Model updating  
 Parametric modeling of damping  
 Damped dynamic systems

## ABSTRACT

All structures exhibit some form of damping, but the characterization of damping is not well-understood, and there is no universal damping model for the dynamic systems. Recently, model updating methods have been used to update or identify the damping matrix in dynamic systems. Most of the finite element updating methods assume viscous and proportional damping models for updating or identifying of damping matrix. In this paper, a new finite element model updating method is proposed in which the damping model is assumed as non-viscous and non-proportional. A parametric exponential non-viscous damping model has been used to model the damping in the dynamic system. The proposed method is the frequency response function (FRF)-based updating model, which updates the non-viscous and non-proportional damping matrix in the dynamic system. The effectiveness of the proposed damped finite element updating method is demonstrated by a numerical example and actual laboratory experiments. First, a numerical study is performed on a cantilever beam structure with non-viscous and non-proportional damping. The numerical study is followed by cases involving actual measured data. Joints and boundary conditions are assumed as a major source of damping, therefore joints and boundary conditions are modelled using relaxation functions and damping coefficients. The updated results have shown that the proposed damped element model updating method can be used to derive accurate models for the non-viscous and non-proportional damped systems. This is illustrated by matching complex FRFs obtained from the updated model with from the experimental data.

## 1. Introduction

All structures exhibit damping, but despite a large body of literature on this subject, damping remains one of the least well-understood aspects of general vibration analysis. The major reason for this is the absence of a universal mathematical model to represent damping forces. The proportional viscous damping model proposed by Rayleigh [1] is commonly used for representing damping in a vibrating system. The Rayleigh damping model assumes that instantaneous generalized velocities are the only variables. The Taylor expansion then leads to a model which encapsulates damping behavior in a dissipation matrix, directly analogous to the mass and stiffness matrices. However, it is important to avoid the misconception that, the Rayleigh damping model is the only model of

\* Corresponding author.

E-mail address: [viar@sdu.dk](mailto:viar@sdu.dk) (V. Arora).<https://doi.org/10.1016/j.jsv.2023.117639>

Received 7 December 2022; Received in revised form 18 February 2023; Accepted 22 February 2023

Available online 26 February 2023

0022-460X/Crown Copyright © 2023 Published by Elsevier Ltd. This is an open access article under the CC BY license (<http://creativecommons.org/licenses/by/4.0/>).

vibration damping. Any model, which guarantees that the energy dissipation rate is non-negative, can be a potential candidate to represent the damping of a given structure. Damping models in which the dissipative mechanism depends on any variable other than the instantaneous velocities are called non-viscous damping models. In broad terms, non-viscous damping mechanisms can be divided into two classes:

- 1 Energy dissipated throughout the bulk material making up the structure which is also called material damping.
- 2 Dissipation of energy associated with junctions or interfaces between parts of the structure, generally called boundary damping.

Material damping can arise from variety of micro-structural mechanisms (Bert, [2]) but for small strains, it is often adequate to represent damping through an equivalent linear, viscoelastic continuum model of the material. Damping can then be considered via the viscoelastic correspondence principle, which leads to the concept of complex moduli. Boundary damping is less easy to model than material or viscous damping, but it is of crucial importance in most of the engineering structures. When damping is measured on a built structure, it is commonly found to be higher in magnitude than the intrinsic material damping of the main components of the structure. This difference is attributed to effects such as frictional micro-slipping at joints. In such a system, the energy loss mechanism is significantly non-linear if examined in detail but can be considered linear (Heckl [3]). When a structure exhibits a damped dynamic behavior that does not conform to the classical and well-known viscous or hysteric damping models, such problems may be addressed by using fractional derivatives leading to a model in terms of general damping parameters. Agrawal and Yuan [4] modeled the damping forces proportional to the fractional derivative of displacements and the fractional differential equations governing the dynamics of a system. Adhikari and Woodhouse [5] proposed a non-viscous damping model in which the dissipation forces depend on the time history of motion, which are represented by convolution integrals between velocities and exponential decay of kernel function.

Damping identification has important applications in many engineering fields such as modal analysis, structural health monitoring, and structural dynamic modifications. Several methods have been developed to identify the damping in the vibrating systems (Lancaster [6]; Minas and Inman [7]). Su et al. [8] experimentally identified exponential damping. Most of the damping identification methods use complex eigendata and are based on the viscous damping model. Moreover, the complex eigendata is very sensitive to experimental errors and errors arising from fitting algorithms. The assumption of viscous damping may not be valid for all real systems and some efforts have been made to identify the non-viscous damping model. Adhikari and Woodhouse [5] identified a non-viscous damping model using complex eigendata. Mondal and Chakraborty [9] also used complex modes arising from a non-proportional dissipative matrix to identify non-viscous damping. Lee and Kim [10] proposed an algorithm for the identification of the damping matrices which identifies the viscous and structural damping matrices of the equation of motion of a dynamic system using the frequency response matrix. Brumat et al. [11] identified both viscous and structural damping matrices using the frequency response functions. The approach requires a full frequency response matrix to identify the damping matrices, but this approach is very expensive both in terms of numerical and experimental effort.

Some research efforts have been made to identify or update the damping matrices using finite element model updating. Finite element model updating techniques have been widely used to reduce the inaccuracies in the finite element models by using the measured data. It is well known that finite element predictions are not accurate because of difficulties in the accurate modeling of boundary conditions, incorrect modeling of joints, and difficulties in modeling of damping, etc. Most of the finite element model updating methods [12–15] neglect damping, so these methods can be used to predict accurately the natural frequencies and real modes in the measured region. But these methods cannot be used for predicting complex frequency response functions (FRFs), amplitudes of vibration, and complex modes. Most of the finite element methods for updating or damping identification are two-step procedure. In the first step, mass and stiffness matrices are updated and in the second step, updated mass and stiffness matrices are used for identification or updating the damping matrix. Yong and Zhenguo [16] proposed a two-step model updating procedure for lightly damped structures using neural networks. In the first step, the mass and stiffness are updated using natural and antiresonance frequencies. In the second step, damping ratios are updated. Pilkey [17] identified the viscous damping matrix using accurate mass and stiffness matrices. Some work has been carried out to update the damping matrices along with mass and stiffness matrices in a single step. Imregun et al. [18] extended the undamped response function method model updating method [18] to update a proportional damping matrix. Arora et al. [19] proposed a damped FE model updating procedure in which both structural and viscous damping matrices are updated along with the mass and stiffness matrices of the dynamic system. Arora et al. [20] proposed a complex parameter-based model updating method in which the finite element model is updated by considering the updating parameters as complex. The imaginary part of the updating parameter is used to develop a structural damping matrix.

All the above-stated damping identification methods work under the assumption that the initial damping model is either viscous or structural damping. Hence, there is a need to develop a method, which can identify the general (non-proportional and non-viscous) damping in dynamic systems. Moreover, most of the damping identification methods do not take the effect of local damping sources for example the presence of joints is the major source of damping in the dynamic system. In this paper, a new FRF-based model updating method is proposed that identifies the non-viscous and non-proportional damping in the dynamic system from the experimental data. The proposed method updates the non-viscous damping matrix along with the mass and stiffness matrices to overcome the problem of complex experimental data. The proposed method can identify the local source of damping in a structure, for example, damping due to the presence of joints, change in material, or damping induced due to the presence of fluid surrounding the structure. To demonstrate the effectiveness of the proposed non-viscous and non-proportional model updating method, numerical and experimental studies are performed. The results show that the proposed finite element model updating method can be used to derive an accurate model of the system. This is illustrated by matching the complex FRFs obtained from the updated model with that from the

experimental data.

## 2. Theory

In this section, the equations for the non-viscous damping model are developed by convolution integrals of the generalized coordinates over appropriate kernel functions. The developed non-viscous damping model is subsequently used in the finite element model updating methodology to develop a new method for non-viscous finite element model updating. The proposed model updating is based on frequency response data. The advantage of the proposed FRF- based model updating method is that it uses measured FRF data directly without requiring any modal extraction. The damping force vector  $f_d$  of a vibrating system is expressed as [5]:

$$f_d(t) = \int_{-\infty}^t G(t-\tau)\dot{x}(\tau)d\tau \tag{1}$$

where  $G$  is an  $N \times N$  matrix of kernel functions and  $x$  is the  $N$ -dimensional vector of displacements. The one-dimensional integral appearing in the above equation is over the time variable  $\tau$  and is independent of the number of degrees of freedom  $N$ . In terms of exponential damping, the kernel function is described by:

$$G(t) = \sum_{k=1}^{k_{max}} C_k \mu_k e^{-\mu_k t}, \quad \text{for } t \geq 0, k = 1, 2, \dots, k_{max} \tag{2}$$

where  $C$  is the viscous damping matrix,  $\mu$  is the relaxation function and subscript  $k$  denotes the number of different exponential models employed to describe the damping behavior of the dynamic system.  $\mu_k$  is used to incorporate local damping mechanism in the dynamic system. The local non-proportional and non-viscous damping is due to the presence of joints, fluid-induced damping, and change in material. The viscously damped system can be expressed as a special case of non-viscous damping, when  $\mu_k \rightarrow \infty$  [21] for the analysis of dynamic systems with general non-viscous damping. The equation of motion reduces to that of a viscously damped system with an equivalent viscous damping.

$$C = \sum_{i=1}^{ne} (\alpha_v)_i (K_{elem})_i + (\beta_v)_i (M_{elem})_i \tag{3}$$

$\alpha_v$  and  $\beta_v$  represent elemental Rayleigh damping coefficients.  $K_{elem}$  and  $M_{elem}$  are elemental stiffness and mass matrices respectively.  $ne$  represents the number of finite elements or groups of elements. Non-proportional damping is obtained by multiplying different damping coefficient values to elemental stiffness and mass matrices. It is easily verified that non-Rayleigh style damping ensues with the simple equation:

$$CM^{-1}K \neq KM^{-1}C \tag{4}$$

Thus, non-viscous damping is a further generalization of classical viscous damping. The kernel function,  $G(\omega)$  in Eq. (2) can be written in the frequency domain as:

$$G(\omega) = \sum_{k=1}^{k_{max}} \frac{\mu_k}{\mu_k + j\omega} C_k \tag{5}$$

where  $j = \sqrt{-1}$ . Thus, the equation of motion with non-viscous damping in the frequency domain can be written as:

$$(K - \omega^2 M + j\omega G)x(\omega) = f(\omega) \tag{6}$$

where  $M$  and  $K$  are system mass and stiffness  $N \times N$  matrices. The receptance frequency response function (FRF) matrix  $R$  of a non-viscous dynamic system can be written as:

$$R = (K - \omega^2 M + j\omega G)^{-1} \tag{7}$$

These non-viscous FRFs are used subsequently for the identification of the non-viscous damping matrix by updating the relaxation function values,  $\mu$  and viscous damping coefficient values ( $\alpha_v$  and  $\beta_v$ ). The following identities relating dynamic stiffness matrix,  $Z$  and receptance FRF matrix,  $R$  for the analytical model and the actual structure, can be written as:

$$Z_{FE} R_{FE} = I \tag{8}$$

$$Z_{EX} R_{EX} = I \tag{9}$$

where the subscripts FE and EX denote the FE model and the experimental model respectively. Expressing  $Z_{EX}$  in Eq. (9) as  $Z_{EX} + \Delta Z$  and then subtracting Eq. (8), the following matrix equation is obtained:

$$\Delta Z R_{EX} = Z_{FE} (R_{FE} - R_{EX}) \tag{10}$$

Pre-multiplying the above equation by  $R_{FE}$  and then using Eq. (7) gives:

$$R_{FE} \Delta Z R_{EX} = R_{FE} - R_{EX} \tag{11}$$

If only one column of the measured FRF matrix  $R_{EX}$  denoted by the vector  $R_{EX_v}$ , is available then the above equation is reduced to:

$$R_{FE} \Delta Z R_{EX_v} = R_{FE_v} - R_{EX_v} \tag{12}$$

Eq. (12) is the basic equation for the FRF-based model updating method. Linearizing  $\Delta Z$  with respect to  $p$ ,  $p = \{p_1, p_2, \dots, p_{nu}\}$ , where  $nu$  is the number of updating parameters, being the vector of updating variables associated with an individual or group of finite elements, gives:

$$\Delta Z = \sum_{i=1}^{nu} \left( \frac{\partial Z}{\partial p_i} \cdot \Delta p_i \right) \tag{13}$$

Dividing and multiplying the above equation by  $p_i$  and then writing  $u_i$  in place of  $\Delta p_i/p_i$ , the equation becomes:

$$\Delta Z = \sum_{i=1}^{nu} \left( \frac{\partial Z}{\partial p_i} \cdot p_i \right) \cdot u_i \tag{14}$$

In the proposed method,  $\Delta Z$  is classified into two categories, that is, physical and damping updating parameters can be written as:

$$\Delta Z = \Delta Z_{pp} + \Delta Z_{dp} \tag{15}$$

where subscripts pp and dp represent physical and damping updating parameters respectively. The physical parameters are used to update the mass and stiffness matrices of the system, whereas, the damping parameters are used to update the non-proportional and non-viscous damping matrix. The damping parameters are further classified as relaxation updating parameters and damping coefficients updating parameters. In the case of relaxation updating parameters  $\mu$ ,  $\Delta Z_\mu$  can be written as:

$$\Delta Z_\mu = j\omega \sum_{n=1}^r \left( \left( \frac{C}{\mu_n + j\omega} - \frac{C\mu_n}{(\mu_n + j\omega)^2} \right) \mu_n \right) \times u_n \tag{16}$$

where subscripts  $r$  represents the total number of updating relaxation parameters. The number of relaxation parameters used in Eq. (16) depends upon the number of different local damping mechanisms considered in the dynamical system. Variation in damping due to change of material, presence of joints and fluid-induced additional local damping. Case studies for these local non-proportional and non-viscous damping have been presented in this paper. Similarly for the case of damping coefficients ( $\alpha_v$  and  $\beta_v$ ) and subscript  $n$  represents the number of updating parameters.  $\Delta Z_{\alpha_v}$  and  $\Delta Z_{\beta_v}$  can be expressed as:

$$\Delta Z_{\alpha_v} = j\omega \sum_{n=1}^{d_1} \left( \left( \frac{C_n}{\mu_n + j\omega} K \right) (\alpha_v)_n \right) \cdot u_n \tag{17}$$

$$\Delta Z_{\beta_v} = j\omega \sum_{n=1}^{d_2} \left( \left( \frac{C_n}{\mu_n + j\omega} M \right) (\beta_v)_n \right) \cdot u_n \tag{18}$$

Eq. (12), after making the substitution for  $\Delta Z$ , can be written at various frequency points chosen from the frequency range considered. The left side of Eq. (12) represents the sensitivity matrix  $S$  given by:

$$S = R_{FE} \Delta Z R_{EX} \tag{19}$$

The selection of frequency points for FRF-based model updating is based on the criteria that the selected frequency points for updating should lie away from the resonance and anti-resonance frequencies [22]. The frequency points are selected manually. A total number of updating parameters ( $nu$ ) is the sum of physical parameters, relaxation ( $r$ ) and damping coefficients parameters ( $d_1$  and  $d_2$ ). The updating parameter vector  $u$ , which consists of the correction factor of physical parameters and damping parameters, is used to update relaxation variables and damping coefficients. The sensitivity matrix is given by:

$$S = \begin{matrix} S(\omega = 1, p = 1)_{N \times N} & S(\omega = 1, p = 2)_{N \times N} & S(\omega = 1, p = 3)_{N \times N} & \dots & \dots & S(\omega = 1, p = nu)_{N \times N} \\ S(\omega = 2, p = 1)_{N \times N} & S(\omega = 2, p = 2)_{N \times N} & S(\omega = 2, p = 3)_{N \times N} & \dots & \dots & S(\omega = 2, p = nu)_{N \times N} \\ S(\omega = 3, p = 1)_{N \times N} & S(\omega = 3, p = 2)_{N \times N} & S(\omega = 3, p = 3)_{N \times N} & \dots & \dots & S(\omega = 3, p = nu)_{N \times N} \\ \vdots & \vdots & \vdots & \dots & \dots & \vdots \\ \vdots & \vdots & \vdots & \dots & \dots & \vdots \\ S(\omega = nf, p = 1)_{N \times N} & S(\omega = nf, p = 2)_{N \times N} & S(\omega = nf, p = 3)_{N \times N} & \dots & \dots & S(\omega = nf, p = nu)_{N \times N} \end{matrix} \tag{20}$$

where  $nf$  is the number of selected frequency points. The sensitivity  $S$  matrix is used to update both physical and damping parameters, which consist of relaxation and damping coefficients.

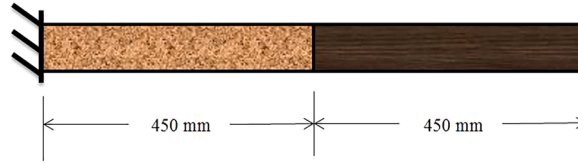


Fig. 1. Cantilever beam made of 2 different materials.

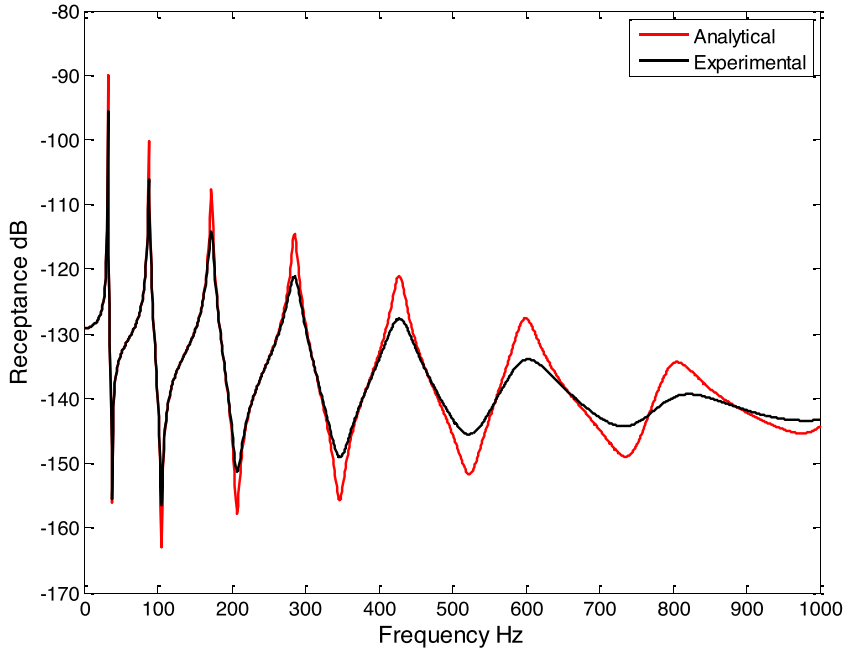


Fig. 2. Overlay of simulated experimental FRF and analytical FRF of cantilever beam.

$$S(\omega)_{((N \times nf) \times nu)} u_{(nu \times 1)} = \Delta R(\omega)_{((N \times nf) \times 1)} \tag{21}$$

The choice of damping relaxation updating parameters  $\mu$  is based on engineering judgment about the possible locations of damping in a structure to ensure that only physical meaningful corrections are incorporated. For damped dynamic structures, the presence of joints, change of material, and the presence of fluid are expected to be the dominant source of non-proportional and non-viscous damping. The proposed method gives non-viscous and non-proportional local damping of the dynamic system. The performance is judged based on the accuracy with which the FRFs predicted by the updated FE model match the experimental FRFs. Practically, the FRFs are available only at a few degrees of freedom which means FRF data is incomplete. In this paper, the coordinate incompleteness has been dealt by using analytically generated FRFs. This has been done by replacing the responses of unmeasured coordinates by analytical counterparts. The process is repeated iteratively until convergence is obtained.

### 3. Case study of a two-material cantilever beam system

A simulated study on a cantilever beam made of 2 different materials is conducted to evaluate the effectiveness of the proposed method. The dimensions of the beam are  $900 \times 50 \times 5$  mm. Half of the beam is made of material 1 and the other half is made of material 2, as shown in Fig. 1. The beam is modeled using thirty (two-noded) beam elements. The displacements in the y-direction and the rotation about the z-axis are taken as the two degrees of freedom at each node. The material properties of materials 1 and 2 are: Material 1: Young’s modulus ( $E_1$ ):  $2 \times 10^{11}$  N/m<sup>2</sup> and density ( $\rho_1$ ): 7800 kg/m<sup>3</sup> Material 2: Young’s modulus ( $E_2$ ):  $0.69 \times 10^{11}$  N/m<sup>2</sup> and density ( $\rho_2$ ): 2700 kg/m<sup>3</sup>. Similarly, different relaxation variables are calculated for the different materials as  $\mu_{X1} = 0.5(2\pi\omega_{n1})$ ,  $\mu_{X2} = 1.1(2\pi\omega_{n2})$  and also the different values for viscous damping matrices for different materials are calculated using  $C_{X1} = (\alpha_v)_{X1} \times K_1 + (\beta_v)_{X1} \times M_1$  N-s/m,  $C_{X2} = (\alpha_v)_{X2} \times K_2 + (\beta_v)_{X2} \times M_2$  N-s/m respectively. The values of the simulated experimental damping coefficients are  $(\alpha_v)_{X1} = 0.00001$ ,  $(\beta_v)_{X1} = 0.1$ ,  $(\alpha_v)_{X2} = 0.00003$  and  $(\beta_v)_{X2} = 0.2$ . The above data is considered simulated experimental data. Error is induced in the analytical model by assuming that the relaxation variable values are:  $\mu_{A1} = 0.3\mu_{X1}$ ,  $\mu_{A2} = 0.5\mu_{X2}$  whereas the viscous damping coefficients of each material are assumed to be:  $(\alpha_v)_A = 0.4(\alpha_v)_x$  and  $(\beta_v)_A = 0.6(\beta_v)_x$ . The analytical FRFs are obtained with known discrepancies in the relaxation variables and damping coefficients. The overlay of the analytical and simulated

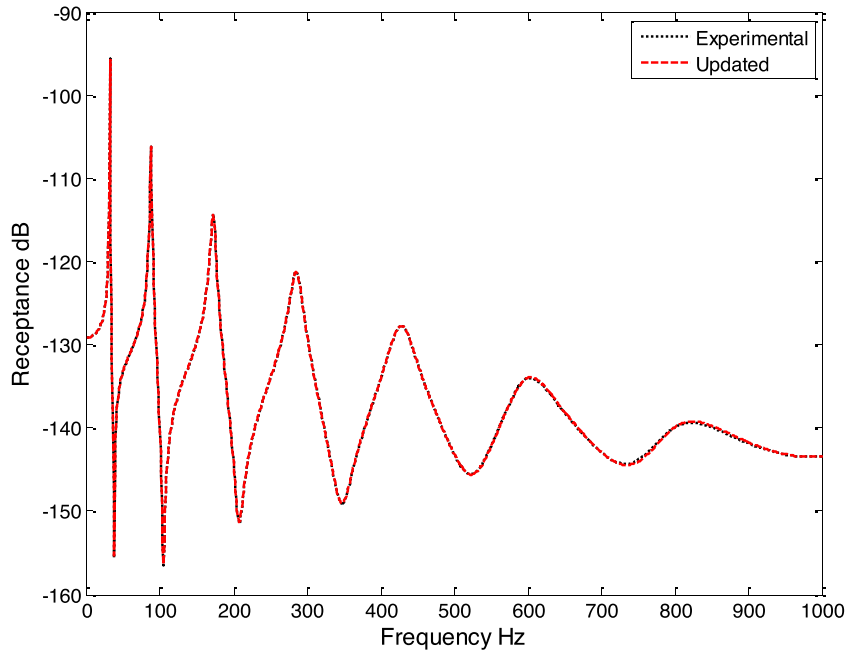


Fig. 3. Overlay of simulated experimental FRF and non-viscous and non-proportional damped updated FRF of cantilever beam structure.

Table 1

Experimental, initial and updated values of relaxation and damping coefficients variable for cantilever beam structure.

Variables	Simulated experimental values	Initial values	Updated values
$\mu_1$	631.12	189.33	631.12
$\mu_2$	38,274	19,137	38,274
$\alpha_{v1}$	0.00001	0.000004	0.00001
$\alpha_{v2}$	0.00003	0.000012	0.00003
$\beta_{v1}$	0.1	0.06	0.1
$\beta_{v2}$	0.2	0.12	0.2

FRFs is shown in Fig. 2. It can be observed from Fig. 2 that the analytical and experimental FRFs don't match at the resonance and anti-resonance frequencies because of the error in the analytical value of the non-viscous damping. The proposed updating method is subsequently applied to update the values of the relaxation function and damping coefficients. The updated and simulated experimental FRFs are plotted in Fig. 3. It can be observed from Fig. 3 that updated and simulated experimental FRFs match completely with each other. The experimental, initial, and updated values of relaxation and damping coefficients variables are given in Table 1. It can be observed from the Table 1 that updated values of the relaxation and damping coefficients variables are same as the simulated experimental values. Similarly, a case study has been carried out by considering high damping in the system. For this case study, values of damping coefficients are changed,  $(\alpha_v)_{x1} = 0.00005$  and  $(\alpha_v)_{x2} = 0.0001$ . Analytical and simulated experimental FRFs and phase angle are plotted in Fig. 4. It can be observed from Fig. 4 that experimental FRF and phase angle plots do not match with each other. After updating, the overlay of the experimental and updated FRFs and phase angle are plotted in Fig. 5 and it can be observed from Fig. 5 that after updating experimental FRF and phase angle matches with the updated FRF and phase angle. It can also be observed that there is a very small error at higher frequencies. To demonstrate the robustness of the proposed method, a case study with 6% noise in the experimental data is also presented. Fig. 6 shows the overlay of the noisy simulated experimental FRF and updated FRF using the proposed method. It can be observed from Fig. 6 that the proposed method can predict experimental FRF accurately and simulated experimental FRF and updated FRF matches completely.

The proposed method can correctly identify the relaxation variables as well as damping coefficients at various levels of noisy data. The success of these cases has proven the feasibility and robustness of the proposed method.

#### 4. Case study of fluid-induced non-viscous damping in monopile structure

In this section, a case study of fluid-induced non-viscous damping in monopile is presented. In the case of the monopile, the water surrounding the structure is the major source of damping. The damping in this case is non-proportional and non-viscous damping. The presence of fluid surrounding a vibrating structure induces additional inertia and damping effect on the structure. The additional inertia induced due to the pressure force of the fluid is called the added mass. The additional damping due to the propagating free

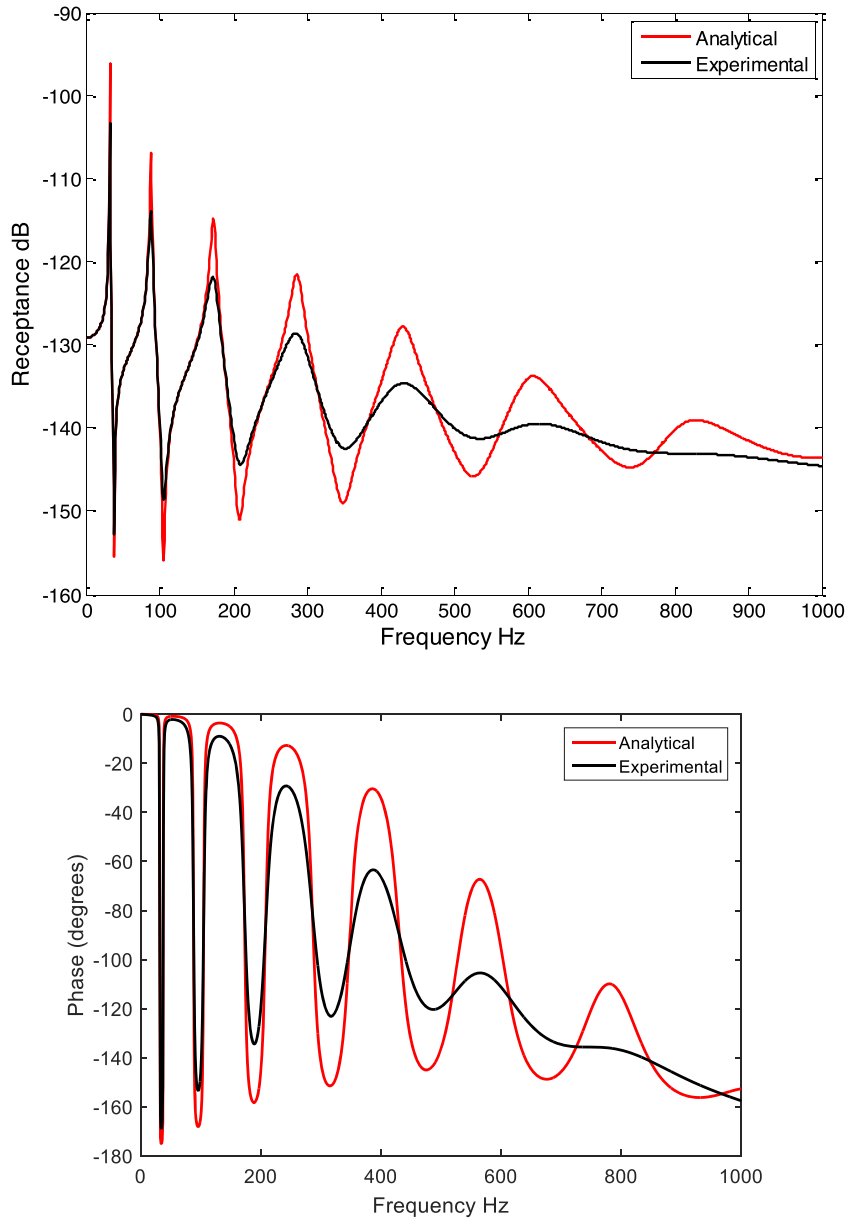


Fig. 4. Overlay of simulated experimental FRF and analytical FRF for the case of highly damped cantilever beam structure.

surface wave, which dissipate the energy is called the radiation or fluid-induced damping [23,24]. One of the earliest to implement this effect were Cummins [25] and Ogilvie [26]. Cummins [25] expressed the fluid-structure interaction in the form of an integro-differential equation. The damping term of the Cummins equation incorporates the memory effect, which is expressed as a convolution integral of the retardation function. The additional contribution in the system dynamics due to the fluid is expressed in terms of potential functions and retardation function in both the mass and damping terms as:

$$(M + M_a)\ddot{x}(t) + \int_t^\infty G(t - \tau)\dot{x}(\tau)d\tau + Kx = p_w(t) \tag{22}$$

where  $M_a$  is the added mass, which depends on the immersed part of the structure and  $\tau_o$  is a time delay.  $G$  is the kernel function, which depends on the forward speed and the geometry of the structure,  $x$  is the displacement and  $p_w$  is the bounded excitation.

In the current study, the fluid force acting on the structure is expressed in terms of the Morison equation [27]. The force acting on monopile, which is partially submerged in water according to Morison's equation is given by:

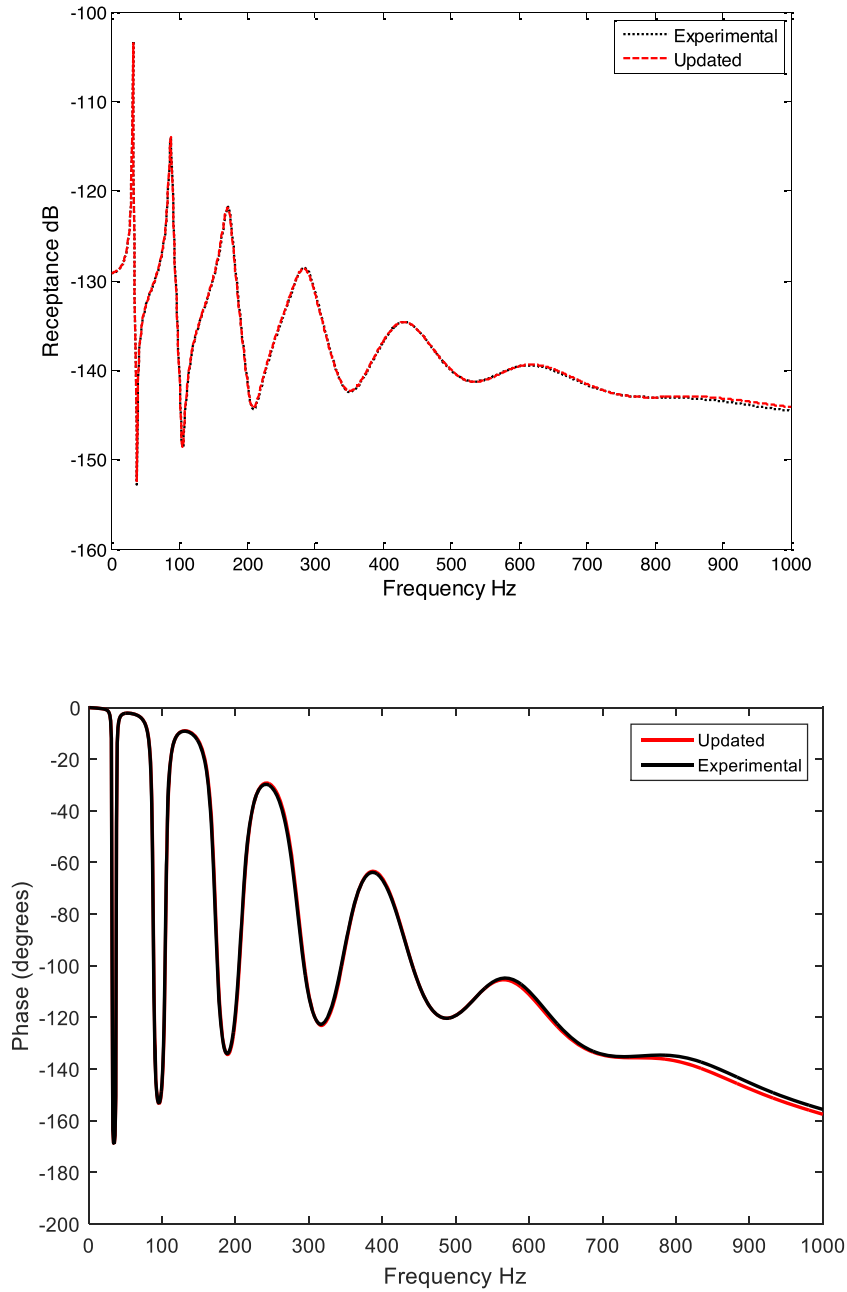


Fig. 5. Overlay of simulated experimental FRF and updated FRF for the case of highly damped cantilever beam structure.

$$F(t) = F_D + F_I + F_{FK} = \frac{1}{2}\rho C_{drag}DL|U - \dot{x}|(U - \dot{x}) + \rho m_i AL(\dot{U} - \ddot{x}) + \rho AL\dot{U} \quad (23)$$

where  $F_D$  is the drag force,  $F_I$  is the inertia force,  $F_{FK}$  is the Froude-Krylov force,  $U$  is the water particle velocity,  $A$  is the cross-sectional area of the monopile,  $L$  is the length of the immersed section of the monopile and  $d\rho$  is the density of water,  $m_i$  is the added mass coefficient, the value of which is 1 for cylinder [25]. Since the modal updating is carried out without external forces from the fluid flow acting on the structure, the water particle velocity terms are neglected. Therefore, the only additional inertia term due to added mass effect is given by:

$$M_a = \rho m_i AL \quad (24)$$

where  $M_a$  is a lumped-mass diagonal matrix. Similarly, the non-linear drag force,  $F_D$  reduces to:

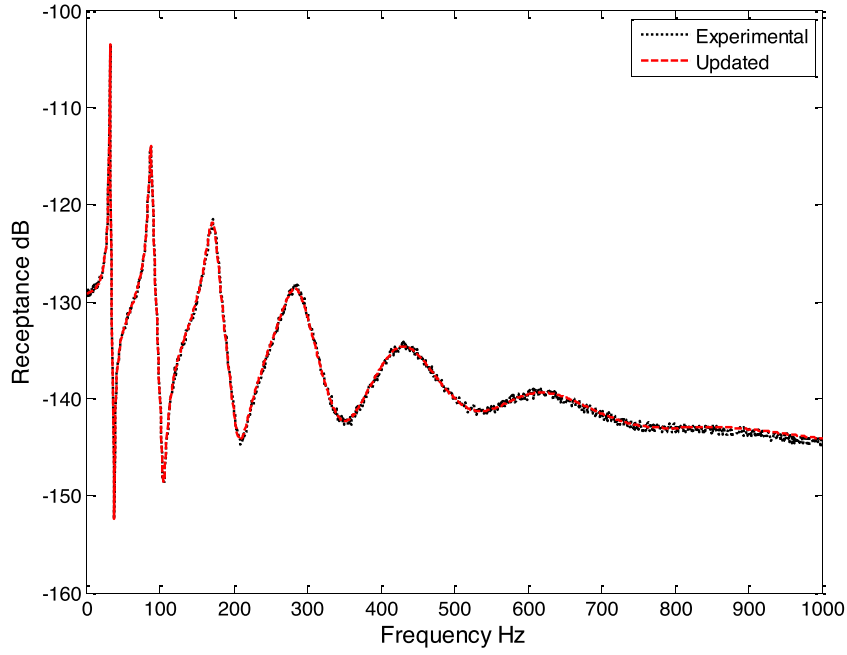


Fig. 6. Overlay of noisy simulated experimental FRF with 6% noise and updated FRF for the case of highly damped cantilever beam structure.

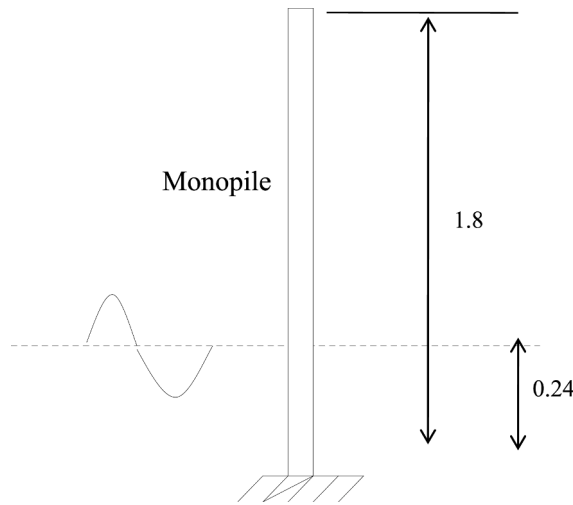


Fig. 7. Monopile structure exposed to wave.

$$F_D = \frac{1}{2} \rho C_{drag} D L \dot{x} |\dot{x}| \tag{25}$$

The drag force can be linearized using equivalent linearization [28,29] under the assumption of Gaussian excitation, which results in viscous non-proportional damping. The resulted damping incorporates the fluid-induced damping effects. Therefore, the effective mass  $M_{eff}$  and damping  $C_{eff}$  matrices in the fluid-induced damped system are given as:

$$M_{eff} = M + M_a \tag{26}$$

$$C_{eff} = C + C_{drag} \tag{27}$$

For the case of fluid-induced damping, the kernel function  $G(\omega)$  given in Eq. (5) is modified as:

$$G(\omega) = \sum_{k=1}^{k_{max}} \frac{\mu_k}{\mu_k + j\omega} C_{effk} \tag{28}$$

**Table 2**  
Dimensions of the monopile considered.

Material Property	Value
Density ( $\rho$ ) $\text{kg m}^{-3}$	8000
Modulus of Elasticity ( $E$ ) $\text{N m}^{-2}$	$2 \times 10^{11}$
Length of monopile m	90
Outer diameter of monopile m	4.5
Inner diameter m	4.4
Depth of immersion m	10.8
Scale ratio	10

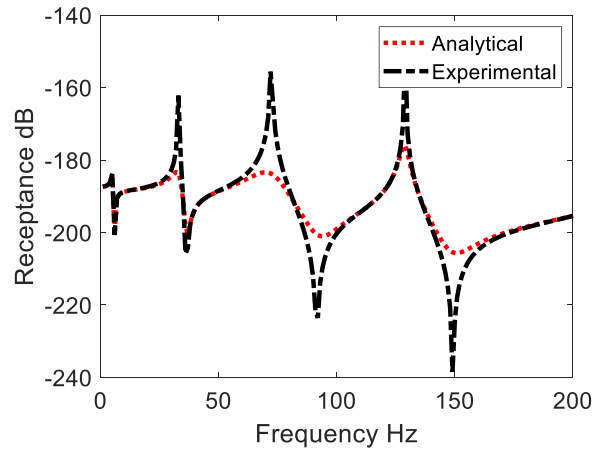


**Fig. 8.** Overlay of simulated experimental FRF and analytical FRF for the case of monopile structure.

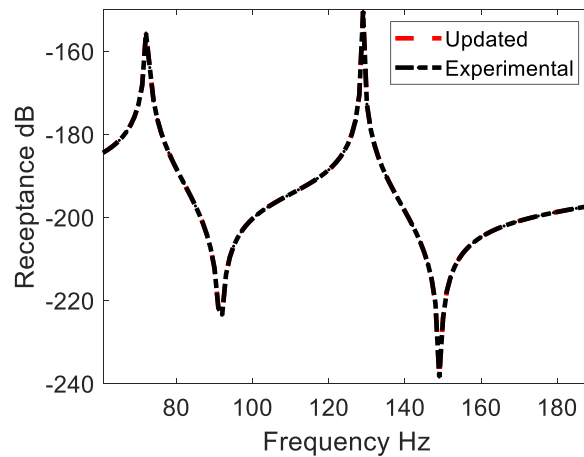


**Fig. 9.** Overlay of simulated experimental FRF and updated FRF for the case of monopile structure.

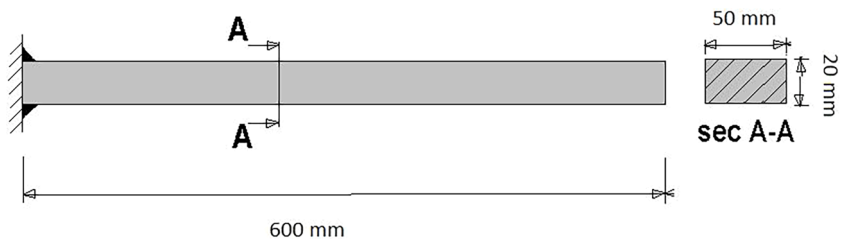


**Fig. 10.** Cantilever beam structure.

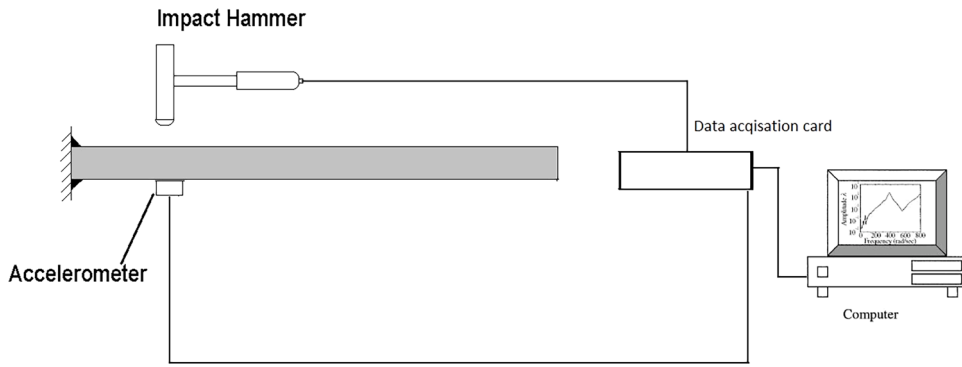


Fig. 11. Instrumentation set-up for modal test using impact excitation.

**Table 3**  
Correlation of measured and FE-model based modal data of beam before updating.

Mode No.	Measured Frequency Hz.	FE-Model Predictions Frequency Hz.	% Error	MAC-Value
1	41.0	46.6	-12.02	0.945
2	258.1	292.6	-11.79	0.972
3	718.4	821.8	-12.58	0.956

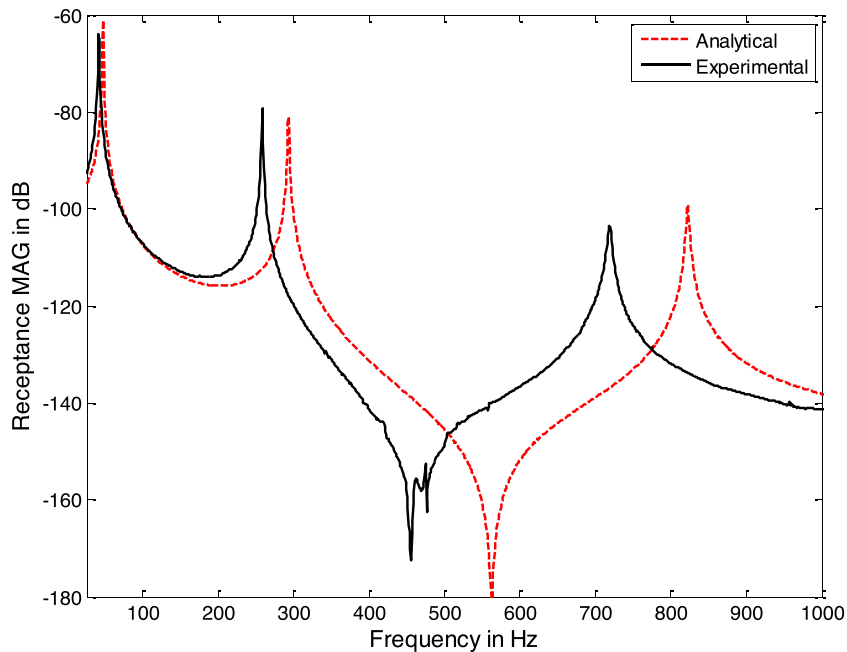


Fig. 12. Overlay of the measured direct FRF and the corresponding finite element model FRF before model updating.

The above-developed methodology is adopted on a scaled model of a monopile structure which could be the tower of an offshore Wind turbine [30] as shown in Fig. 7. The dimensions of the Monopile structure are given in Table 2. The monopile is modeled as a Euler Bernoulli cantilever beam of cylindrical cross section. Added mass terms are included in the mass matrix up to the depth of submergence. The added mass coefficient of cylinder is taken as 1. The finite element model of the monopile is developed using 25 beam elements in which it is assumed that 3 elements are submerged in the water. Since the radiation damping and the memory effect is contributed from the submerged part of the monopile most of the energy dissipates in this region. Therefore, the value of relaxation variable changes from zero for above water to non-viscous for submerged portion given by  $\mu_x = 0.05(2\pi\omega n_1)$ . The damping coefficients for submerged part are assumed constant with  $\alpha_v = 0.00001$  and  $\beta_v = 0.001$ . The analytical damping model is assumed to be viscous by assigning very high value to the relaxation variable that is  $\mu_A = 2 \times 10^4 \mu_x$ . A comparison between the analytical and simulated

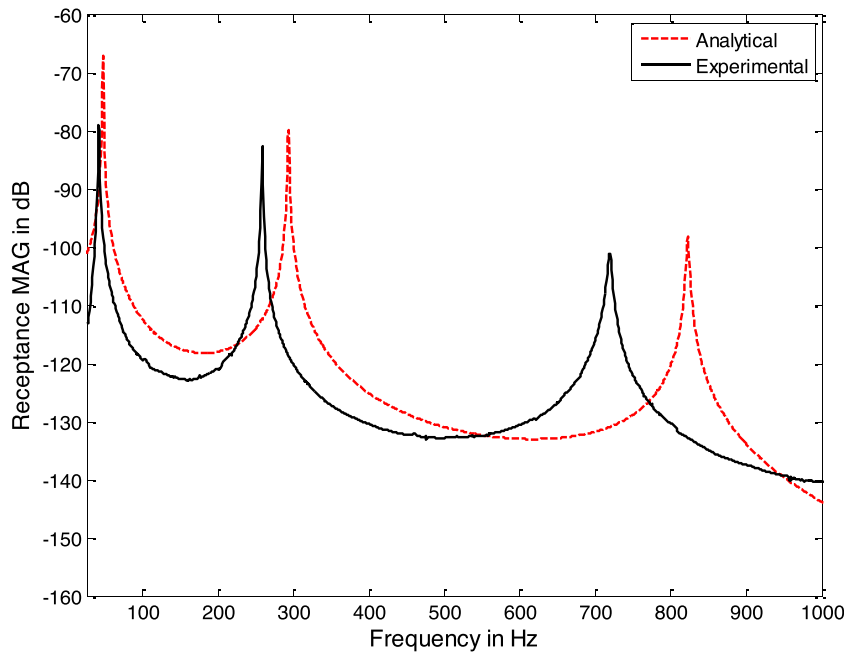


Fig. 13. Overlay of the measured cross FRF and the corresponding finite element model FRF before model updating.

Table 4

Values of each spring stiffness and relaxation variables at the fixed end of cantilever beam before and after updating.

Updating variable	Initial Value	Updated values
$K_x$	$3.28 \times 10^6$	$1.41 \times 10^5$
$K_y$	$3.28 \times 10^6$	$1.53 \times 10^5$
$K_r$	$3.28 \times 10^6$	$1.89 \times 10^5$
$\mu_x$	57.8	715.1
$\mu_y$	57.8	710.2
$\mu_r$	57.8	982.5

experimental FRFs are plotted in Fig. 8 indicates mismatch in the FRF amplitudes. After updating the relaxation parameter, the overlay of the experimental and updated FRFs are providing better fit as shown in Fig. 9. It can be concluded from this case study that the proposed method can successfully be applied in the cases, where fluid is the major source of damping in the system. In this case damping dominantly is non-proportional and non-viscous.

### 5. Case study of cantilever beam structure using experimental data

An experimental study on an aluminum cantilever beam is also conducted to evaluate the effectiveness of the proposed method. The dimensions of the beam are  $600 \times 50 \times 20$  mm as shown in Fig. 10. The beam is modeled using five, beam elements (one translational degree of freedom in y direction and one rotational degree of freedom) and the fixed end is modeled by taking coincident nodes. Thus, two nodes that are geometrically coincident are taken as fixed end instead of one node. A horizontal, a vertical and a rotational spring couples two nodes at each of such coincident pair of nodes and the stiffness of these springs is  $K_x$ ,  $K_y$  and  $K_r$  respectively. Initially, the value of relaxation variable ( $\mu$ ) is considered the same for all the finite elements including spring elements. The value of  $\mu$  is calculated using the first analytical natural frequency as  $\mu_{x1} = 0.2(2\pi\omega_{n1})$ . Whereas very low damping coefficients values are used for modeling the damping matrix as  $\beta_v = 0.0001$  and  $\alpha_v = 0.00005$ . The instrumentation set-up used to perform the modal test on the cantilever beam structure using impact excitation is shown in Fig. 11. The responses are measured at one location by accelerometer while the structure is excited with an impact hammer at five locations, thus 5 FRFs are acquired. From the acquired FRFs, the modeshapes are calculated in the frequency range of 0–1000 Hz. The correlation between the finite element (FE) and the experimental modal data is given in Table 3. An overlay of the measured FRF and the corresponding FE model FRF at the cross and direct locations are shown in Figs. 12 and 13. It can be observed from Table 3 and Figs. 12 and 13 that the FE model is in error. For better correlation between the experimental and FE model, the damping matrix and stiffnesses at the fixed end of the cantilever beam are updated using the proposed non-viscous damping method. The choice of updating parameters is based on engineering judgment about the possible locations of modeling errors in a structure is one of the strategies to ensure that only physical meaningful corrections

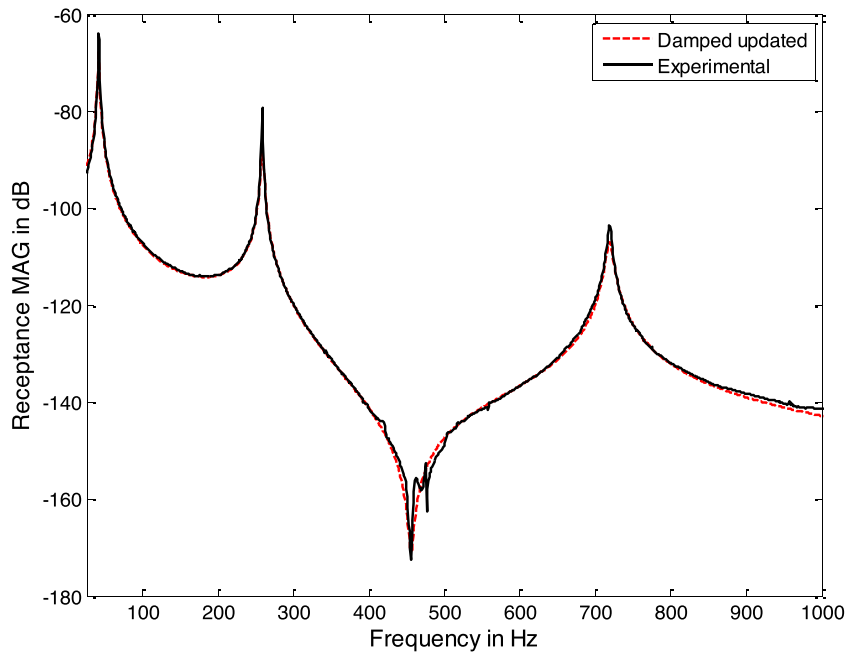


Fig. 14. Overlay of the measured dry FRF and the corresponding finite element model FRF after model updating using proposed method.

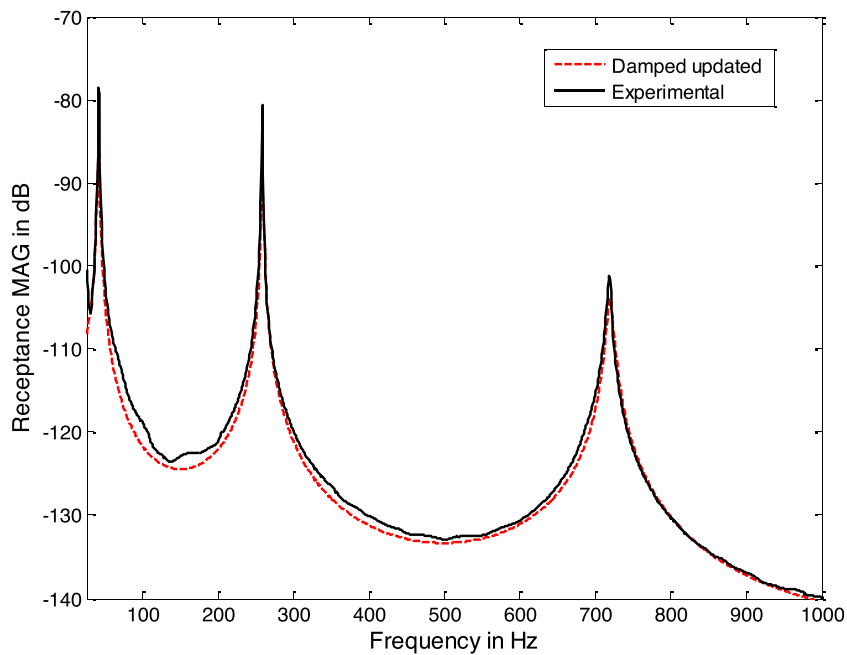


Fig. 15. Overlay of the measured cross FRF and the corresponding finite element model FRF after model updating using proposed method.

Table 5

Correlation of measured and FE-model based modal data of cantilever beam after updating using proposed method.

Mode No.	Measured Frequency Hz.	After updating Frequency Hz.	% Error	MAC-Value
1	41.0	41.0	0	0.954
2	258.1	258.1	0	0.966
3	718.4	718.0	.06	0.973

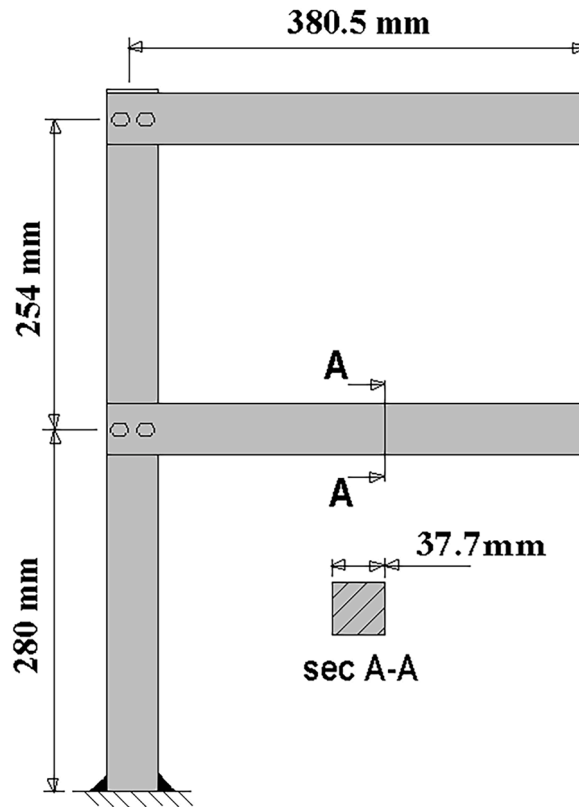


Fig. 16. F-shaped structure.

are made. In the case of cantilever beam structure, modeling of damping and stiffness at the fixed end are expected to be the dominant source of inaccuracy in the FE model. The 3 spring stiffnesses, 6 damping coefficients and 3 relaxation variables at the fixed end are chosen as updating variables. The initial and final values of 3 springs and 3 relaxation variables at the fixed end are given in Table 4. It is observed that the values of stiffness of all the springs at the fixed end are reduced and values of the three springs are not very different from each other whereas the values of relaxation variables increase after updating. Figs. 14 and 15 show the overlay of measured and non-viscous damped updated FRFs. It can be observed from Fig. 14 and 15 that the shape of the updated FRFs is same as that of measured FRFs. The correlation between the updated model and measured modal data is presented in Table 5. It can be observed from Table 5 that the updated model using the proposed method is able to predict the measure modal data accurately.

An experimental case study of a cantilever beam structure has been carried out to show the effectiveness of the proposed non-viscous and non-proportional model updating method. In this case, it is assumed that the fixed end of the cantilever beam structure is the major source of error in the finite element model and a major source of damping in the structure. Stiffnesses, relaxation variables and damping coefficients at the fixed end are updated. The success of the proposed method is demonstrated by matching the updated FRFs with experimental FRFs. The proposed method is working well for the case of experimental data of cantilever beam structure.

## 6. Case study of F-shape structure using experimental FRF data

An experimental study on an F-shape structure resembling a drilling machine is also conducted to evaluate the effectiveness of the proposed method. The F-shape structure has been constructed by bolting the two beam members horizontally to a vertical beam member, which in turn, has been welded to the base plate at the bottom. All the beam members have a square cross-section with 37.7 mm side as shown in Fig. 16. A finite element model of the F-structure is built, as shown in Fig. 17, using 48 two-dimensional frame elements (Two translational degrees of freedom in  $x$  and  $y$  direction and one rotational degree of freedom, per node) to model in-plane dynamics. In the F- shaped structure, there are three joints, which are modeled by taking coincident nodes at each of them. Thus, two nodes that are geometrically coincident are taken as joint instead of one node. A horizontal, a vertical, and a rotational spring couple the two nodes at each of such a coincident pair. The stiffnesses of these springs are  $K_x$ ,  $K_y$  and  $K_r$  respectively. The modal test is performed by exciting the structure with an impact hammer at 16 locations and the response is measured at one location using an accelerometer. A comparison of the corresponding experimental and analytical natural frequencies, the percentage difference between them, and the corresponding Modal assurance criteria (MAC) value for the first five modes are given in Table 6. An overlay of the measured FRFs and the corresponding FE model FRFs are shown in Fig. 18. It is observed that the shape of the FE model FRF curve is similar to the measured curve. It, therefore, infers that though the FE model is in error it is, in principle, of updatable quality.

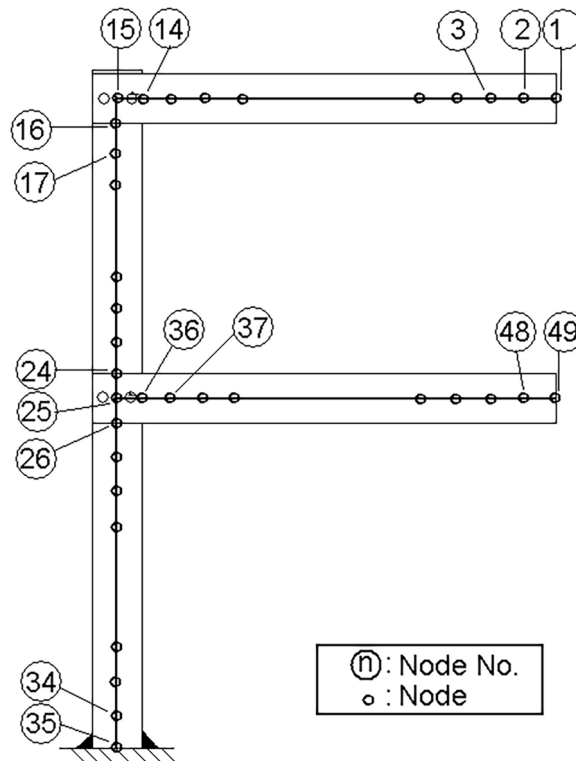


Fig. 17. Initial FE model.

**Table 6**  
Correlation of measured and FE-model based modal data of F-shaped structure before updating.

Mode No.	Measured Frequency in Hz.	FE-Model Predictions			Updated model Predictions		
		Frequency in Hz.	% Error	MAC-Value	Frequency in Hz.	% Error	MAC- Value
1	34.95	43.05	23.17	0.9231	34.25	-2.0	0.9923
2	104.02	123.67	18.89	0.9016	100.27	-3.60	0.9693
3	133.96	185.21	38.26	0.9281	134.42	0.34	0.9675
4	317.52	385.17	21.30	0.9141	313.73	-1.19	0.9423
5	980.16	1020.06	4.07	0.7108	973.44	-0.68	0.4370

In the case of F-structure, modeling joint stiffnesses are expected to be a dominant source of inaccuracy in the FE model assuming that the values of material and the geometric parameters are correctly known. Analytical sensitivity analysis of the joint springs shows that the rotational stiffness is the most important variable affecting the FRFs. Rotational springs of stiffness  $K_{r1}$ ,  $K_{r2}$  and  $K_{r3}$  coupling the rotational degrees of freedom of the coincident nodes at the three joints are taken as physical updating parameters. The other two degrees of freedom of the coincident nodes are taken as rigidly coupled. The joints are the major source of energy dissipation (Bert [2]). Therefore, it is also assumed that these joints are the major source of energy dissipation or damping in the structure. The joints' damping coefficients and relaxation functions related to all the rotational stiffnesses of each joint are considered damping updating parameters. The frequency points are selected for model updating manually by avoiding both resonance and anti-resonance frequencies. The frequency points selected for updating of F-shape structure are 27, 31, 99, 101, 131, 311, 442, 515, and 825 Hz for each of the FRFs. The initial and final values of the rotational spring stiffness of each joint are given in Table 7. It can be observed from Table 7 that the values of stiffness of the rotational springs corresponding to three joints are reduced and values of the three springs are not very different from each other while the damping coefficients and relaxation variables values of each rotational spring stiffness represent damping in the system. A comparison of the correlation between the measured and the updated model natural frequencies is given in Table 6. It can be observed from Table 6 that the proposed method can predict accurately natural frequencies and MAC-values. The major reason for the deterioration of the MAC value concerning mode five is that there are close modes. Table 8 shows the initial and updated values of the damping parameters, and it can be observed from the Table 8 that updated relaxation variable values represent non-viscous damping in the structure. Fig. 19 shows the overlay of measured and updated FRF obtained using the proposed method and FRF obtained using the viscous damping identification method [31]. It can be observed from Fig. 19 that the proposed non-proportional and non-viscous damping updating method can predict the experimental FRFs more accurately than the viscous damping identification method.

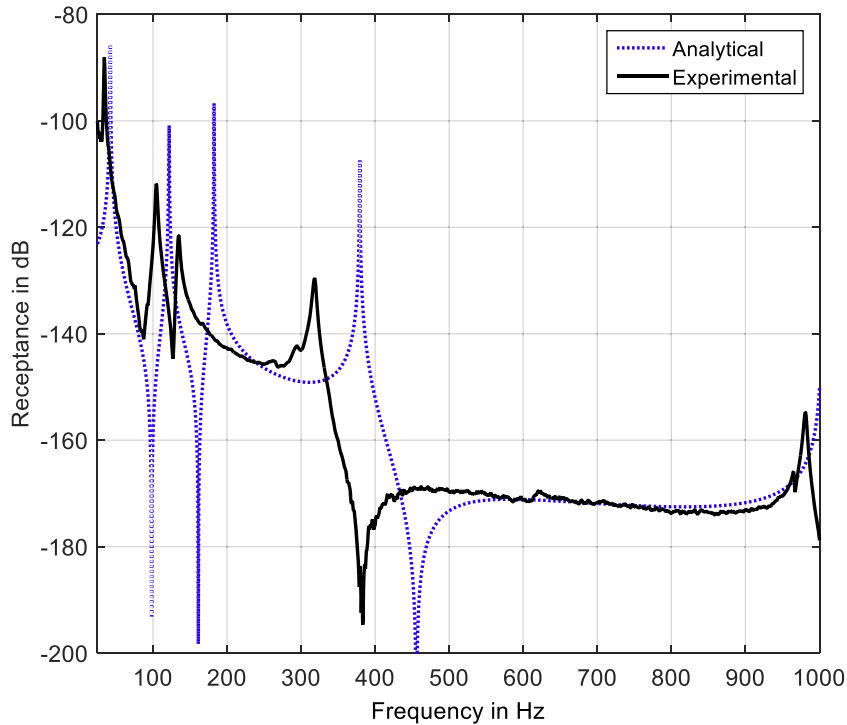


Fig. 18. Overlay of the measured FRF and the corresponding FE model FRF of F-shaped structure before updating.

Table 7

Values of physical updating parameters of the F-shaped structure before and after updating.

Updating Variable	Initial Value (N m rad <sup>-1</sup> )	Updated values using extended damped RFM (N m rad <sup>-1</sup> )
K <sub>r1</sub>	3.28E+06	2.61E+05
K <sub>r2</sub>	3.28E+06	2.69E+05
K <sub>r3</sub>	3.28E+06	3.15E+05

Table 8

Values of damping updating parameters of the F-shaped structure before and after updating.

Updating variable	Initial Value	Updated values
$\alpha v_{r1}$	$1 \times 10^{-4}$	$2.31 \times 10^{-2}$
$\alpha v_{r2}$	$1 \times 10^{-4}$	$1.87 \times 10^{-2}$
$\alpha v_{r3}$	$1 \times 10^{-4}$	$2.05 \times 10^{-2}$
$\mu_{r1}$	100	22.56
$\mu_{r2}$	100	25.22
$\mu_{r3}$	100	38.43

### 7. Conclusions

A new finite element model updating method in which damping is considered non-viscous and non-proportional is proposed. An exponential non-viscous and non-proportional damping model has been used to model the damping in the dynamic system. The proposed FE model updating method is a frequency response function (FRF)-based updating model which updates the non-viscous and non-proportional damping matrix in the dynamic system by parametric approach. The novel aspects of this paper include:

- The proposed method is a single-step method in which the damping matrix is updated along with non-damping (mass and stiffness) matrices, whereas most other FE model updating methods for the damped system are two-step methods. In the first step, mass and stiffness matrices are updated and in the second step, updated mass and stiffness matrices are used to identify the damping matrix.
- In the proposed method, identified damping matrix is non-proportional and non-viscous by using relaxation functions and damping coefficients as updating damping parameters.

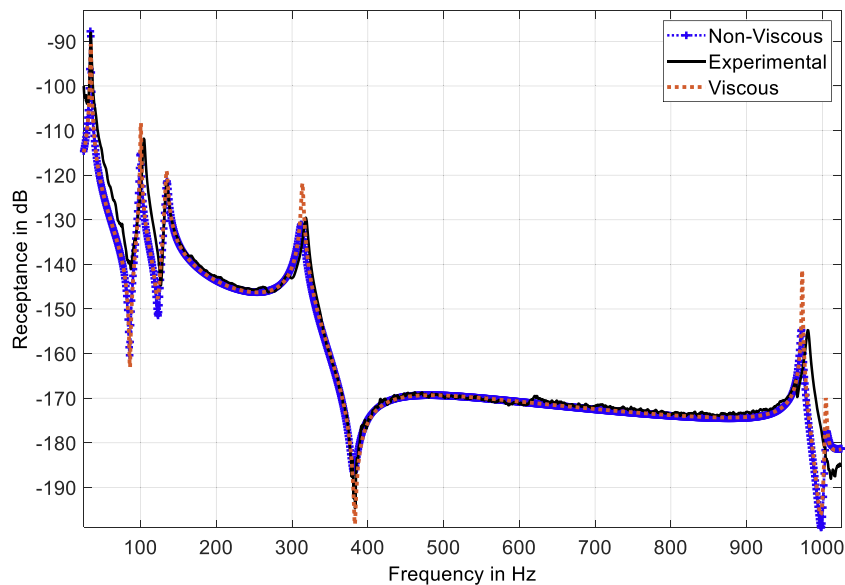


Fig. 19. Overlay of the measured FRF and the corresponding FRF using proposed non-proportional and non-viscous method and viscous method [34].

- The proposed method can be used for identifying the local damping in a structure by parametric modeling of the joints and boundary conditions using relaxation functions and damping coefficients.
- The proposed method addresses the difficulties of updating a non-viscous and non-proportional damping matrix using complex FRF data.

The proposed method is working successfully for the cases of simulated numerical data as well as experimental data. To check the robustness of the proposed method, various levels of noise are introduced in the simulated data. The proposed method can identify the damping accurately in presence of noisy data. The proposed method is applied to the experimental data of a cantilever beam and F-shape structures in which the joint stiffnesses, relaxation variables and damping coefficients are updated. The success of these cases has proven the feasibility of the proposed method.

#### Credit authorship contribution

**Vikas Arora:** Writing and editing draft, Software, Investigation, Formal analysis, Experimentation, Data analysis.

**Sondipon Adhikari:** Conceptualization, Software, Investigation, Methodology, Formal analysis, Writing-review editing draft

**Kiran Vijayan:** Conceptualization, Software, Investigation, Methodology, Formal analysis, Writing-review & editing draft

#### Declaration of Competing Interest

None.

#### Data availability

No data was used for the research described in the article.

#### References

- [1] Lord Rayleigh, *Theory of Sound (two volumes)*, Dover Publications, 1897.
- [2] C.W. Bert, Material damping: an introduction review of mathematical models, measures and experimental techniques, *J. Sound Vib.* 29 (1973) 129–153.
- [3] M. Heckl, Measurements of absorption coefficients of plates, *J. Sound Acoust. So. America.* 34 (1962) 803–808.
- [4] O.P. Agrawal, L. Yuan, A numerical scheme for dynamic systems containing fractional derivatives, *J. Vib. Acoust.* 124 (2002) 321–324.
- [5] S. Adhikari, J. Woodhouse, Identification of damping part 2, non-viscous damping, *J. Sound Vib.* 243 (2000) 63–88.
- [6] P. Lancaster, Expression for damping matrices in linear vibration, *J. Aero. Sc.* 28 (1961), 256–256.
- [7] C. Minas, D.J. Inman, Identification of viscous damping in structure from modal information, *J. Vib. Acoust.* 113 (1991) 219–224.
- [8] L. Su, S.Q. Mei, Y.H. Pan, Y.F. Wang, Experimental identification of exponential damping for reinforced concrete cantilever beams, *Eng. Struct.* 186 (2019) 161–169.
- [9] S. Mondal, S. Chakraborty, Identification of non-proportional viscous damping matrix of beams by finite element model updating, *J. Vib. Cont.* 24 (2018) 2134–2148.

- [10] J.H. Lee, J. Kim, Development and validation of a new experimental method to identify damping matrices of a dynamic system, *J. Sound Vib.* 246 (2001) 505–524.
- [11] M. Brumat, J. Slavič, M. Boltežar, Spatial damping identification in the frequency domain—A theoretical and experimental comparison, *J. Sound Vib.* 376 (2016) 182–193.
- [12] M. Baruch, Optimization procedure to correct stiffness and flexibility matrices using vibration data, *AIAA J.* 16 (1978) 1208–1210.
- [13] A. Berman, E.J. Nagy, Improvement of a large analytical model using test data, *AIAA J.* 21 (1983) 927–928.
- [14] J.D. Collins, G.C. Hart, T.K. Hasselman, B. Kennedy, Statistical identification of structures, *AIAA J.* 12 (1974) 185–190.
- [15] R.M. Lin, D.J. Ewins, Analytical model improvement using frequency response functions, *Mech. Syst. Signal Process.* 8 (1994) 437–458.
- [16] L. Yong, T. Zhengu, A two-level neural network approach to dynamic FE model updating including damping, *J. Sound Vib.* 275 (2004) 931–952.
- [17] D.F. Pilkey, D.J. Inman, M.I. Friswell, The direct updating of damping and stiffness matrices, *AIAA J.* 36 (1998) 491–493.
- [18] M. Imregun, K.Y. Sanliturk, D.J. Ewins, Finite element model updating using frequency response function data-II: case study on a medium size finite element model, *Mech. Syst. Signal Process.* 9 (1995) 203–213.
- [19] V. Arora, S.P. Singh, T.K. Kundra, Further experience with model updating incorporating damping matrices, *Mech. Syst. Signal Process.* 24 (2010) 1383–1390.
- [20] V. Arora, S.P. Singh, T.K. Kundra, Damped model updating using complex updating parameters, *J. Sound Vib.* 320 (2009) 438–451.
- [21] S. Adhikari, N. Wagner, Direct time-domain approach for exponentially damped systems, *Comp. Struct.* 82 (2004) 2453–2461.
- [22] K.S. Kwon, R.M. Lin, Frequency selection method for FRF-based model updating, *J. Sound Vib.* 278 (2004) 285–306.
- [23] M.E. McCormick, *Ocean Engineering mechanics: With Applications*, Cambridge University Press, 2009.
- [24] O. Faltinsen, *Sea Loads On Ships and Offshore Structures*, 1, Cambridge University Press, 1993.
- [25] W.E. Cummins, *The Impulse Response Function and Ship Motion*, Report 1661, Department of the Navy, David W. Taylor Model Basin, Hydromechanics Laboratory, Research and Development Report, 1962.
- [26] T.F. Ogilvie, Recent progress toward the understanding and prediction of ship motions, in: *Proc. 5th ONR Symp. on Naval Hydrodynamics*, 1964.
- [27] T. Sarpkaya, *Wave Forces On Offshore Structures*, Cambridge University Press, 2010.
- [28] K. K. Vijayan, C.R. Barik, O.P. Sha, Shock transmission through universal joint of cutter suction dredger *Oce. Eng.* 233 (2021), 109185.
- [29] J.B. Roberts, P.D. Spanos, *Random Vibration and Statistical Linearization*, Courier Corporation, 2003.
- [30] B.W. Byrne, G.T. Hously, Foundations for offshore wind turbines, *Philos. Trans. R. Soc. London A* 361 (2003) 2909–2930.
- [31] V. Arora, S.P. Singh, T.K. Kundra, Finite element model updating with damping identification, *J. Sound Vib.* 324 (2009) 1111–1123.